Proc. of the Conference "Applications of Physics in Mechanical and Material Engineering" (APMME 2020)

Effect of Cooling Rate on Glass Forming Ability of Novel Fe-Based Bulk Metallic Glass

H. Redaei, P. Rezaei-Shahreza*, A. Seifoddini and S. Hasani

Department of Mining and Metallurgical Engineering, Yazd University, 89195-741, Yazd, Iran

Doi: 10.12693/APhysPolA.138.265 *e-mail: parisarezaei88@yahoo.com

In the present study, the effect of cooling rate on the glass forming ability of $Fe_{41}Co_7Cr_{15}Mo_{14}Y_2C_{15}B_6$ bulk metallic glass was investigated. For this purpose, three samples with a mentioned nominal composition were prepared with diameters of 2 mm in water-cooled copper, and 2.5 mm and 3 mm in graphite molds. The amorphicity of the samples were confirmed by X-ray diffraction (XRD). Also, thermal behavior of the glassy samples was evaluated with a differential scanning calorimeter (DSC) from ambient to 1200 °C. The characteristics temperatures, such as the glass transition temperature (T_g), the onset temperature of crystallization (T_x), solidus (T_m), and liquidus (T_l) temperatures were determined by using DSC curves. The results calculated by using the various criteria (i.e., $T_{rg} = T_g/T_l$, $\omega = (T_g/T_x) - (2T_g/(T_l + T_g))$, $\delta = T_x/(T_l - T_g)$, and New $\beta = (T_x \times T_g)/(T_l - T_x)^2)$ revealed that the thermal stability of this BMG was increased by decreasing the cooling rate. On the other hand, Tang's isoconversional method was used to determine the activation energy of crystallization in these samples. These results confirmed that activation energy of crystallization process was increased by decreasing the cooling rate, which was in good agreement with that were calculated by various criteria. Finally, an increase in the GFA can be related to the formation of clusters in the amorphous matrix with a decrease in the cooling rate and thus change the chemical composition of the amorphous matrix.

topics: bulk metallic glasses (BMGs), glass forming ability (GFA), kinetics, isoconversional method, activation energy

1. Introduction

Among all of the BMG alloy systems, Fe-based BMGs have attracted considerable attention due to the combination of low material cost [1–4], excellent mechanical properties [5, 6], good corrosion resistance [7, 8], high fracture strength [9–11] and soft magnetic properties [12–17]. Also among these alloys, amorphous iron alloy has a maximum critical thickness of 16 mm which increases its thermal stability [18–20]. One way of producing this class of alloys is to create in situ nanocomposites using lower cooling rates such as using graphite molds, which can significantly increase their thermal stability. Therefore, the use of this method to improve glass forming ability (GFA) has attracted the attention of many researchers [21, 22]. In fact, the cooling rate control is one of the most important factors during the casting process [23]. Therefore, in this paper, the effect of cooling rate on the glass forming ability and crystallization kinetics of $Fe_{41}Co_7Cr_{15}Mo_{14}Y_2C_{15}B_6$ glassy alloy is investigated. Furthermore, thermal properties and the nature of the amorphous structure of specimens were investigated by differential scanning calorimetry (DSC) and X-ray diffraction (XRD), respectively.

2. Material and method

Alloy ingots of composition of bulk metallic glass $Fe_{41}Co_7Cr_{15}Mo_{14}Y_2C_{15}B_6$ were prepared by arc melting furnace with purities of over 99.99% in a highly purified argon atmosphere. The mass losses were measured for each ingot after melting less than 0.2 mass%. Each prealloy ingot was remelted several times to ensure chemical uniformity. Then, amorphous alloys were produced by injection casting in a copper mold with diameter of 2 mm (C2) and graphite mold with 2.5 (G2.5) and 3 mm (G3) in diameter and 70 mm in length. The amorphous nature of the as-cast samples were examined by X-ray diffraction (XRD, X'Pert MPD Philips diffractometer) with CuK_α radiation ($\lambda = 0.1540$ nm). The thermal properties were performed using differential scanning calorimetry (DSC) at the heating rate of 20 K/min from ambient to 1200 °C with argon flow.

3. Results and discussion

Figure 1 shows the XRD patterns of the as-cast $Fe_{41}Co_7Cr_{15}Mo_{14}Y_2C_{15}B_6$ amorphous alloys in different molds and diameters and molds casting. As one can see, only a broad diffuse peak

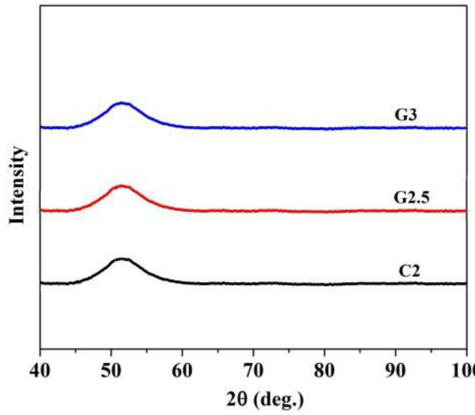

Fig. 1. XRD pattern of the as-cast investigated amorphous alloys.

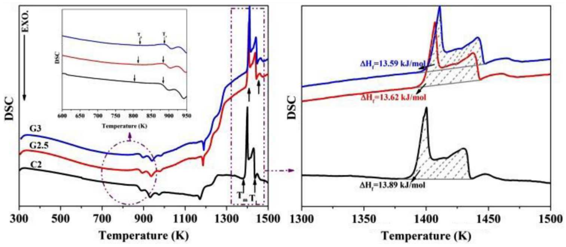

Fig. 2. DSC curves related to the alloy investigated at the heating rate of 20 K/min.

TABLE I

Summary of thermal parameters of the investigated BMGs, extracted from DSC curves.

Sample code	Diameter [mm]	T_g [K]	T_x [K]	T_m [K]	T_l [K]
C2	2	789	883	1385	1438
G2.5	2.5	813	882	1387	1440
G3	3	818	881	1389	1441

TABLE II

The value of parameters of GFA for the investigated alloys.

Sample code	Criteria			
	T_{rg}	New β	δ	ω
C2	0.55	2.26	1.36	0.18
G2.5	0.56	2.30	1.40	0.20
G3	0.57	2.31	1.42	0.21

TABLE III

The other method for calculated GFA.

Sample code	ΔG [kJ/mol]	E_P [kJ/mol]	Free volume [J/g]
C2	2.54	560 ± 12	267
G2.5	2.49	561 ± 10	232
G3	2.47	561 ± 11	225

at $2\theta = 50°$ is observed without any detectable sharp peak. The thermal properties of these alloys were examined by thermal analysis.

Figure 2 presented the DSC curves of the as-cast $Fe_{41}Co_7Cr_{15}Mo_{14}Y_2C_{15}B_6$ amorphous alloy in continuous heating condition at heating rate of 20 K/min. According to Fig. 2, the DSC curve of all specimens shows four exothermic and endothermic peaks related to the crystallization stages and melting process, respectively.

The critical temperatures of each sample such as the glass transition temperature (T_g), onset temperature of crystallization (T_x), solidus (T_m), and liquidus (T_l) temperatures are listed in Table I. According to their values — the T_g shifts to higher temperatures as the cooling rate decreases. On the other hand, it is shown that the values of the glass forming ability criteria reported in Table II, such as T_{rg}, New β, δ, and ω and G3, increase in G2.5 and G3 samples compared to C2 samples, and thus the crystallization is delayed. In addition, the increase in apparent activation energy (E_p) that is obtained by the Tang's isoconversional method [24], confirms the increase of GFA by reducing the cooling rate (as one can see in Table III).

Another method of calculating the thermal stability of bulk metallic glasses is to determine the Gibbs free energy difference (ΔG_c) between the undercooled melt and the crystalline phases in the amorphous alloy, which is inversely correlated with the GFA. The ΔG_c of these alloys is expressed by (1) of Battezzati and Garrone [25]:

$$\Delta G_c = \frac{\Delta H_f \Delta T}{T_m} - \tau \Delta S_f \left[\Delta T - T \ln\left(\frac{T_m}{T}\right)\right], \quad (1)$$

where ΔH_f is the fusion enthalpy (kJ/mol), τ is the proportionality coefficient usually taken as 0.8 for metallic glass-forming liquids. The other quantities are defined as $\Delta T = T_m - T$ [K] and $\Delta S_f = \Delta H_f / T_m$ [kJ/(mol K)]. It is worth notice that parameter $0.8T_m$ is usually used as T [19]. The ΔG_c can also be expressed as follows [19]:

$$\Delta G_c = 0.1828 \Delta H_f. \quad (2)$$

In the present $Fe_{41}Co_7Cr_{15}Mo_{14}Y_2C_{15}B_6$ alloys, ΔG_c is calculated to be 2.54, 2.49, and 2.47 kJ/mol for the C2, G2.5, and G3 alloys, respectively, (see Table III). The ΔG_c decreases with the decreasing cooling rate and ultimately increases thermal stability. Another way to evaluate the GFA of these alloys is to calculate the free volume. The free volume related to the both the exothermic relaxation below T_g and the height of the glass transition peak [26]. According to Table III, less atomic movement will result in small free volume and entropy, thereby reducing cooling rates to include more thermal stability [18]. In other words, the results revealed that decreasing the cooling rate and the presence of clusters by changing the chemical composition locally leads to an increase of GFA [27, 28].

4. Conclusion

In the present work, we investigated the effect of cooling rate on the glass forming ability of the $Fe_{41}Co_7Cr_{15}Mo_{14}Y_2C_{15}B_6$ amorphous alloys. Therefore, the samples were prepared with diameter of 2 mm in water-cooled copper, and 2.5 mm and 3 mm in graphite molds. The results showed that with decreasing cooling rate and free volume, the glass transition temperature increased. As a result, thermal stability increases. The reason for this can be attributed to the formation of clusters in the amorphous matrix and the change of the local chemical composition with a decrease in cooling rate. Thus, the sample with a diameter of 3 mm in graphite mold has the highest glass forming ability.

References

[1] J. Zbroszczyk, J. Olszewski, W. Ciurzyńska, M. Nabiałek, P. Pawlik, M. Hasiak, A. Łukiewska, K. Perduta, *J. Magn. Magn. Mater.* **304**, e724 (2006).

[2] Q. Chen, D. Zhang, J. Shen, H. Fan, J. Sun, *J. Alloys Compd.* **427**, 190 (2007).

[3] T. Bitoh, D. Watanabe, *Metals (Basel)* **5**, 1127 (2015).

[4] Q.J. Chen, J. Shen, H.B. Fan, J.F. Sun, Y.J. Huang, D.C. McCartney, C. Qing-Jun, S. Jun, F. Hong-Bo, S. Jian-Fei, H. Yong-Jiang, *Chinese Phys. Lett.* **22**, 1736 (2005).

[5] P. Rezaei-Shahreza, A. Seifoddini, S. Hasani, *J. Alloys Compd.* **738**, 197 (2018).

[6] P. Rezaei-Shahreza, A. Seifoddini, S. Hasani, *Thermochim. Acta.* **652**, 119 (2017).

[7] T. Bitoh, A. Makino, A. Inoue, *Mater. Trans.* **44**, 2020 (2003).

[8] K. Arai, N. Tsuya, M. Yamada, T. Masumoto, *IEEE Trans. Magn.* **12**, 939 (1976).

[9] J. Zhang, W. Wang, G. Li, H. Ma, J. Qin, X. Bian, *Trans. Nonferrous Metall. Soc. China* **20**, 71 (2010).

[10] D.M. Minic, D.M. Minic, T. Zák, P. Roupcová, B. David, *J. Magn. Magn. Mater.* **323**, 400 (2011).

[11] D.M. Minić, D.G. Minić, A. Maričić, *J. Non. Cryst. Solids.* **355**, 2503 (2009).

[12] M. Hasiak, K. Sobczyk, J. Zbroszczyk, W. Ciurzynska, J. Olszewski, M. Nabiałek, J. Kaleta, J. Swierczek, A. Łukiewska, *IEEE Trans. Magn.* **44**, 3879 (2008).

[13] K. Błoch, M. Nabiałek, *Acta Phys. Pol. A*, **127**, 413 (2015).

[14] J. Olszewski, J. Zbroszczyk, K. Sobczyk, W. Ciurzyńska, P. Bragiel, M. Nabiałek, J. Świerczek, M. Hasiak, A. Łukiewska, *Acta Phys. Pol. A* **114**, 1659 (2008).

[15] M. Nabiałek, *Arch. Metall. Mater.*, **61**, 439 (2016).

[16] K. Jez, B. Jez, P. Pietrusiewicz, *Rev. Chim.* **70**, 3158 (2019).

[17] B. Jez, *Rev. Chim.* **68**, 1903 (2017).

[18] S. Hasani, P. Rezaei-Shahreza, A. Seifoddini, M. Hakimi, *J. Non. Cryst. Solids.* **497**, 40 (2018).

[19] J. Gondro, K. Bloch, M. Nabialek, S. Garus, *Mater. Technol.* **50**, 559 (2016).

[20] K. Gruszka, M. Nabiałek, K. Błoch, S. Walters, *J. Mater. Res.* **106**, 689 (2015).

[21] R. Srivastava, J. Eckert, W. Loser, B. Dhindaw, L. Schultz, *Mater. Trans.* **43**, 1670 (2002).

[22] R. Tang, B. Zhou, Y. Ma, F. Jia, X. Zhang, *Mater. Res.* **18**, 3 (2015).

[23] P. Ramasamy, A. Szabo, S. Borzel, J. Eckert, M. Stoica, A. Bárdos, *Sci. Rep.* **6**, 35258 (2016).

[24] W. Tang, Y. Liu, H. Zhang, C. Wang, *Thermochim. Acta.* **408**, 39 (2003).

[25] Y. Ji, S. Pang, T. Zhang, *J. Alloys Compd.* **505**, 497 (2010).

[26] C. Schuh, T. Hufnagel, U. Ramamurty, *Acta Mater.* **55**, 4067 (2007).

[27] C. Gammer, B. Escher, C. Ebner, A.M. Minor, H.P. Karnthaler, J. Eckert, S. Pauly, C. Rentenberger, *Sci. Rep.* **7**, 44903 (2017).

[28] B. Zheng, Y. Zhou, J.E. Smugeresky, E.J. Lavernia, *Metall. Mater. Trans. A.* **40**, 1235 (2009).